NUCLEAR STRUCTURE FAR OFF STABILITY — RISING CAMPAIGNS*

M. Górska[a], A. Banu[a], P. Bednarczyk[a,b], A. Bracco[c], A. Bürger[d]
F. Camera[c], E. Caurier[e], P. Doornenbal[a,f], J. Gerl[a], H. Grawe[a], M. Honma[g]
H. Hübel[d], A. Jungclaus[h], A. Maj[b], G. Neyens[i], F. Nowacki[e], T. Otsuka[j]
M. Pfützner[k], S. Pietri[l], Zs. Podolyák[l], A. Poves[h], P.H. Regan[l], P. Reiter[f]
D. Rudolph[m], H.J. Wollersheim[a]

and the RISING Collaboration

[a]Gesellschaft für Schwerionenforschung (GSI), Planckstr. 1, Darmstadt, Germany
[b]H. Niewodniczański Institute of Nuclear Physics, Kraków, Poland
[c]Dipartimento di Fisica, Universita di Milano, 20133 Milano, Italy
[d]Helmholtz-Institut für Strahlen- und Kernphysik, Universität Bonn, Germany
[e]IPHC, 67037 Strasbourg Cedex 2, France
[f]Institut für Kernphysik, Universität zu Köln, 50937 Köln, Germany
[g]University of Aizu, Fukushima 965-8580, Japan
[h]Departamento de Física Teórica, Universidad Autonoma de Madrid, Spain
[i]Katholieke Universiteit Leuven, 3001 Leuven, Belgium
[j]Department of Physics and Center for Nuclear Study, University of Tokyo, Japan
[k]Institute of Experimental Physics, Warsaw University, Poland
[l]Department of Physics, University of Surrey, Guildford, GU2 7XH, UK
[m]Department of Physics, Lund University, 22100 Lund, Sweden

(Received December 1, 2006)

Nuclear structure studies at GSI attracted recently increased interest for the results of present activities as well as for the future project FAIR. A broad range of physics phenomena can be addressed by high-resolution in-beam γ-ray spectroscopy experiments with radioactive beams offered within the Rare Isotopes Spectroscopic INvestigation at GSI (RISING) project. It combined the EUROBALL Ge-Cluster detectors, the MINIBALL Ge detectors, the HECTOR-BaF detectors, and the fragment separator FRS. The secondary beams produced at relativistic energies were used for Coulomb excitation or secondary fragmentation experiments to study projectile like nuclei by measuring de-excitation photons. The first results of the "fast beam campaign" is discussed in comparison to various shell model calculations. The discussion focuses on the $N = 32, 34$ sub-shell closure based on neutron rich Cr isotopes. Alternatively, the relativistic radioactive beams, both in their ground and isomeric states, were implanted and their decay could be investigated. The "stopped beam campaign" has started in October 2005 with a series of g-factor measurements. It continued from February 2006 with the next configuration and the main goal of identification of new isomers and angular momentum population in fragmentation reactions.

PACS numbers: 21.10.–k, 21.60.Cs, 23.20.–g, 25.60.–t

* Presented at the Zakopane Conference on Nuclear Physics, September 4–10, 2006, Zakopane, Poland.

1. Introduction

The CLUSTER [1] detector part of the EUROBALL array is presently used at GSI to explore exotic nuclei with radioactive beams. The SIS/FRS [2] facility provides secondary beams of unstable rare isotopes after fragmentation reactions or secondary fission of relativistic heavy ions with sufficient intensity for in-beam gamma-ray spectroscopy measurements. Following a workshop held in November 2000 at GSI, the RISING collaboration has been initiated to pursue this project. Secondary beams arrive to the secondary target/stopper either in the ground state or, if existing, in high spin isomeric states which are long lived enough to survive the flight path through the FRS. The beams have been used so far either *(i)* at high energies ($\geq$ 100 MeV/u) for relativistic Coulomb excitation and fragmentation reactions or *(ii)* stopped for isomeric decay studies. The letter of intent summarizing the proposed physics and the intended experimental technique of the RISING project is available [3].

The physics of experiments performed in the first RISING campaign, which is the main topic of this paper, exploit unique beams at relativistic energies in the range from 100 to 600 MeV/u [4]. Those experiments which depend on fragmentation products from heavy primary beams are only feasible at GSI. The RISING spectrometer was employed not only for relativistic Coulomb excitation but also for pioneering high-resolution γ-spectroscopy experiments after secondary nucleon removal reactions and secondary fragmentation. Several of the performed experiments focused on new methods and techniques in order to determine magnetic moments and life times of short lived states, properties of isomeric states and spectroscopic factors at relativistic energies for the first time.

2. RISING campaigns

The experimental program at RISING has been and will be performed in different campaigns requiring dedicated specifications of the experimental setup.

- In the **Fast-beam campaign** intermediate energy Coulomb excitation was used to measure the $B(E2; 0^+ \rightarrow 2^+)$ in neutron-rich $^{56-58}$Cr [5], light ^{108,112}Sn [6], and shape coexistent ^{134}Ce, ^{136}Nd [7]. In secondary fragmentation of ^{55}Ni and ^{37}Ca [8] mirror symmetry in the pf and sd shells was studied. Further experiments comprise knockout reactions in ^{132}Sn, sub-picosecond lifetime measurements following fragmentation of ^{34}Si, and collective modes in ^{68}Ni. The selected results from the fast beam campaign are further described and discussed in this paper.

- In the *g*-**RISING campaign** employing passive stoppers for implantation, running at GSI in 2005, experiments on *g*-factors of isomeric states around ^{132}Sn produced in fission as well as in fragmentation, and proton-rich ^{192}Pb were performed. Spin-alignment studies will enable to extend these experiments from fragmentation products to neutron-rich high-energy fission fragments [9].
- As a sensitive probe of shell structure changes, new isomers have been investigated within the **Stopped-beam campaign** started in 2006. The studies concentrated on $N = Z$ nuclei below ^{56}Ni where the 10^+ isomer in ^{54}Ni was identified with a proton decay branch, nuclei below ^{100}Sn where the isomers in $N = Z$ ^{82}Nb and ^{86}Tc were identified for the first time yielding information on the isospin $T = 0$ and $T = 1$ competing levels, and neutron-rich $N = 126$ isotones below ^{208}Pb where among others a (10^+) isomer in ^{204}Pt has been identified. A bulk of nuclear structure information was obtained from the fission and fragmentation studies of the $A = 132$ mass region where a number of isomeric states was found in Ag, Cd, In isotopes including an (8^+) isomer in ^{130}Cd and a core excited state in ^{131}In. More information on the performed experiments can be found in other contributions to this conference, *i.e.* [10–14] and the forthcoming papers [15, 16]. An experiment planned for December 2006 searches for X(5) symmetry candidates around $A = 110$.
- In the future stopped-beam campaign an **Active Stopper** will be used, dedicated for β-decay and μs-isomer studies of shape evolution below ^{208}Pb and K-isomers from ^{190}W to ^{170}Dy, of the Gamow–Teller resonance and isomers in ^{100}Sn and of isospin symmetry in weak and strong interactions in the $N = Z$ daughters of ^{54}Ni, ^{50}Fe and ^{46}Cr.

3. Physics interest of the fast beam campaign

The motivations to explore nuclear structure of exotic nuclei at relativistic beam energies focus on (a) shell structure of unstable doubly magic nuclei and their vicinity, (b) isospin symmetry along the $N = Z$ line and mixed symmetry states, (c) shapes and shape coexistence and (d) collective modes and E1 strength distribution.

3.1. Shell structure

Spectroscopic data on the single particle structure of unstable doubly magic nuclei and their nearest neighbours are indispensable for theoretical description of the effective interactions in large-scale shell-model calculations [17]. The studies around the $N = Z$ doubly magic nuclei ^{56}Ni and ^{100}Sn provide an excellent probe for single-particle shell structure, proton–neutron interaction and the role of correlations, normally not treated in mean

field approaches. The $B(E2; 0^+ \rightarrow 2^+)$ values in semi-magic Sn nuclei provide a sensitive test for changing (sub)shell structure, the E2 polarisability and the shape response of the magic core. For several reasons conventional techniques, employing (HI,xn) reactions, are very difficult or even impossible and the proposed Coulomb excitation measurements are the only way to obtain the information needed to investigate the evolution of shell structure close to the proton drip line. Beyond the very neutron-rich shell closures from ^{34}Si to ^{132}Sn the possible disappearance of the familiar Woods–Saxon shell closures and their reappearance as harmonic magic numbers is predicted by several mean-field calculations [18]. Moreover, ^{78}Ni and ^{132}Sn are located close to the astrophysical rapid neutron capture process path and indirect evidence for an altered shell structure and shell quenching of magic gaps at $N = 82$ and $N = 126$ is derived from recent r-process network calculations [19]. Alternatively, observed new shell structure in light and medium-heavy nuclei can be qualitatively understood in terms of monopole shifts of selected nucleon orbitals, with deviating predictions for new shell gaps and spin-orbit splitting [20, 21]. So far the investigative methods have not been able to gather information in the region of neutron-rich Ni and Sn isotopes concerning the most significant interaction matrix elements, the magnetic moments and the spectroscopic factors, which are sensitive indicators of their structure.

3.2. Symmetries

The validity of the isospin symmetry for the strong interactions is a fundamental assumption in nuclear physics. The degree to which this symmetry holds as the proton drip line is approached, remains an open question. Experimentally, the symmetry shows as nearly identical spectra in pairs of mirror nuclei obtained by interchanging protons and neutrons. A slight breakdown of the symmetry arises from the Coulomb interaction, causing small differences in excitation energies between isobaric analog states. The Coulomb energy differences between excited analog states in mirror nuclei have been studied for proton rich ($N = Z - 2$) isobars in the $A = 50$ region revealing subtle nuclear structure effects as a function of spin and energy [22].

Within the framework of the proton–neutron version of the interacting boson model (IBM-2) the existence of low-lying valence shell excitations, which are not symmetric with respect to the proton–neutron degree of freedom, are predicted. These states are called mixed-symmetry states and are *e.g.* established in all stable $N = 52$ isotones [23, 24].

3.3. Shapes

The phenomenon of shape coexistence is caused by various structure effects, which can be traced back to the polarisation by high spin intruder orbitals, which happens to occur primarily in exotic regions of the chart of

nuclides. Along semi-magic isotopic and isotonic chains, midway between shell closures ($N = 82$ and $N = 126$), $2p - 2h$ and $4p - 4h$ proton core excitations into high-spin orbitals cause coexistence of spherical, oblate and prolate shape as seen in the Pb ($Z = 82$) isotopes. States observed experimentally have no firm assignment of the specific shape so far [25]. Aided by shell gap melting, even the ground state may become deformed as in the well known $N = 20$ nucleus ^{32}Mg [26]. High-K isomers, built by multi-quasi particle configurations, due to their influence on the amount of pairing and/or collectivity left, may give rise to shape changes. Most often deformed nuclei obey axial and reflection symmetry. However, in specific nuclear regions where the Fermi level approaches pairs of close lying, opposite-parity orbitals with $\Delta j = \Delta l = 3$ reflection asymmetric shapes are predicted, *e.g.* the heavy Ba nuclei may show octupole deformed states.

3.4. Collective excitations

Collective excitations such as the giant dipole resonance (GDR), built from collections of single-particle excitations are necessarily influenced by the nuclear shell structure. In exotic nuclei like $^{68-78}$Ni the proton–neutron asymmetry may give rise to changes in the shell structure. Theoretical calculations predict a significant change in the GDR strength distribution as one progresses towards the doubly magic ^{78}Ni. The excitation function of the isovector GDR mode is expected to fragment substantially, favoring a redistribution of the strength towards lower excitation energies. Measurements of the GDR strength function provide access to the isospin dependent part of the in-medium nucleon–nucleon interaction and on dipole type vibrations of the excess neutrons. The predicted low-energy shift of the GDR strength was confirmed in neutron-rich oxygen isotopes by the LAND group at GSI by means of virtual photon absorption measurements [27]. The GDR experiment in ^{68}Ni applied a complimentary method, virtual photon scattering, which relies on real projectile γ-ray emission following the virtual excitation. In order to observe discrete γ-transitions with high resolution and γ-decay from the GDR, the RISING array was augmented by BaF scintillators. Further details on the GDR measurement in ^{68}Ni are given in Ref. [28].

4. Experimental technique

The γ-ray spectroscopy of nuclei produced from exotic beams is performed after in-flight isotope separation. The exotic beams are produced by fragmentation of a heavy stable primary beam or fission of a ^{238}U beam on a ^{9}Be or ^{208}Pb target, in front of the fragment separator, FRS.

4.1. Particle identification and tracking

The FRS was operated in a standard achromatic mode, which allows a separation of the species of interest by combining magnetic analysis with energy loss in matter. The transmission through the FRS is typically 20–70% (depending on the mass region) for fragmentation and 1–2% for fission. The separated ions are identified on an event-by-event basis with respect to mass and atomic number via combined time-of-flight, position tracking, and energy loss measurement. This is achieved with plastic detectors, multi-wire proportional chambers and a MUSIC ionisation chamber. Details on the secondary beam identification are given in Ref. [4]. After passing the identification set-up, the radioactive ions at relativistic energies are focussed onto a secondary target. Massive slits reduce the amount of unwanted species reaching the secondary target.

Behind the target the calorimeter telescope, CATE, is used for the exit channel selection. CATE consists of position sensitive Si ΔE detectors (laboratory angular range $\pm 3^\circ$) and CsI scintillators for total energy measurement. The performance of secondary fragment identification detector is described in Ref. [29].

4.2. Gamma-ray detection

For the excited fragments moving at a high velocity ($v/c = 0.43$ at the fragment energy of $100\,\mathrm{MeV}/u$) the Cluster γ-ray detectors have to be positioned at either forward or backward angles in order to minimize Doppler broadening. A photo of the γ-ray detection setup is shown in Fig. 1.

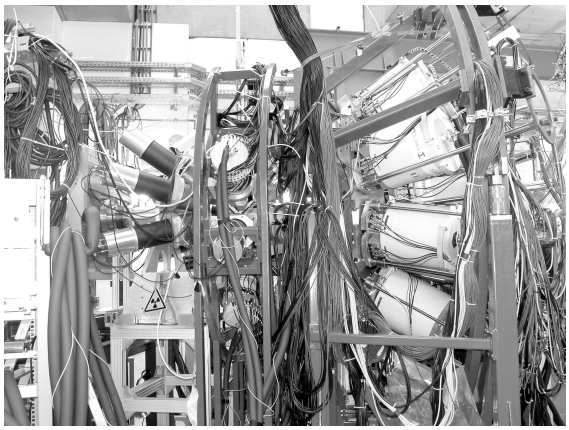

Fig. 1. The RISING fast beam set-up including Euroball-Cluster, Miniball [30] and Hector [31] detector arrays at the final focus of the FRS. The beam enters from the left.

The distance to the target depends on the required energy resolution. The best possible configuration of the 15 Cluster detectors placed in three rings available for experiments with fast beams is displayed in Fig. 2.

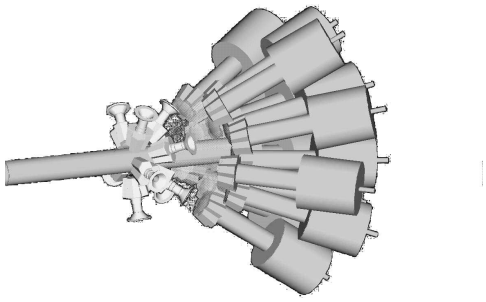

Fig. 2. Schematic picture of the Ge detector arrays used in the RISING fast beam campaign. The Miniball detectors are shown at about 90° angles (without LN_2 supply) and Cluster detectors at forward angles.

Due to the Lorentz boost the main efficiency contribution among the Cluster detectors comes from the first ring. This ring was positioned to achieve 1.5% resolution. The 5 Clusters in the 2nd and 3rd rings could be moved closer to the target position, for an increased efficiency but a lower overall resolution of 2.05% at 1.3 MeV. If both rings are placed at a minimum distance of 70 cm then the configuration reaches a total efficiency of 2.5% while the average weighted energy resolution is only slightly increased to 1.88%. The segmentation of the Miniball detectors [30] allows to place them at shorter distance and larger angles as seen in Fig. 2 not affecting the resolution significantly but contributing strongly to the total γ-ray efficiency to about 6%. The on-line analysis of the data is performed with the CRACOW software [32].

5. The $N = 32, 34$ sub-shell closure

The experimental evidence for changing shell structure along the very neutron-rich $N = 8, 20$ and 28 isotones can be explained by the monopole part of the nucleon–nucleon interaction [20, 21, 33]. It is traced back to the tensor interaction [34–36] which is strongly binding for nucleons in spin-flip configurations with $\Delta l = 0$ (spin–orbit partners) and $\Delta l = 1, 2$ in adjacent major shells in the $T = 0$ (proton–neutron) channel of the two-body interaction. It is specifically strong for optimum radial overlap, *i.e.* identical number of nodes in the radial wave function. The effect was first discussed for the p, sd and pf shells [20, 21, 33] with shell gaps changing from the HO magic neutron number $N_{\rm m} = 8, 20, 40$ to $N_{\rm m} - 2N_{\rm HO} = 6, 16(14), 34(32)$, with $N_{\rm HO}$

counting the harmonic oscillator quanta. The ambiguity for $N_{\rm HO} > 1$ is due to the presence of $j = 1/2$ orbits as *e.g.* $s_{1/2}$ or $p_{1/2}$, which have a strong $T = 1$ (pairing) monopole opening another gap when these shells are filled.

The neutron-rich Cr isotopes are located at a key point on the pathway from the $N = 40$ sub-shell closure via a deformed region to spherical $N = 28$ isotones. Experimentally a possible $N = 32$ shell develops in the 2^+ excitation energy of Ca isotopes and a maximum in this signature is also observed for Ti and Cr, while the Ni isotopes show constant 2^+ energies. Three experiments were performed to measure Coulomb excitation of high-energy ^{54}Cr, ^{56}Cr and ^{58}Cr beams with the RISING setup, where the known $B(E2; 2^+ \rightarrow 0^+)$ in ^{54}Cr served as a reference to reduce possible systematic errors. Details of the experimental results are given in Ref. [5].

The extracted $B(E2; 2^+ \rightarrow 0^+)$ and $E(2^+)$ systematics of the Ti [37] and Cr [5] isotopes has been extensively discussed in comparison to different shell model calculations KB3G [38] and GXPF1/GXPF1A [39, 40] (see *e.g.* [33]). The polarization charge used in those calculation for protons and neutrons was 0.5 e. The local peak in the experimental $N = 32$ $E(2^+)$ and a corresponding minimum in $B(E2; 2^+ \rightarrow 0^+)$, both in the Cr and Ti isotpes systematics was observed. A confirmation of these results for ^{56}Cr and ^{54}Ti was recently obtained in the plunger measurement at the Köln Tandem accelerator [41].

Closer inspection of the shell model results, which all show a rather flat behaviour with respect to shell structure, indicates that the $N = 32$ gap between $p_{1/2}$ and $p_{3/2}$ stays constant when moving from Ca to Cr into the

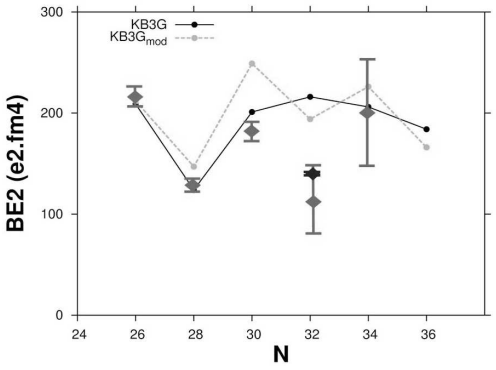

Fig. 3. Comparison of the experimental and theoretical $B(E2 : 2^+ \rightarrow 0^+)$ values for Cr isotopes. The influence of using different neutron effective charge [43] in the calculations is shown in two different curves for the KB3G (light grey) and KB3G$_{\rm mod}$ (black) interaction. The experimental points are shown in dark grey. The recent result [41] (see text) is shown in black.

proton shell while the $N = 34$ gap between $p_{3/2}$ and $f_{5/2}$ reduces strongly in the GXPF1/GXPF1A [39, 40] and disappears for KB3G [38]. Furthermore, using in the KB3G calculation the effective charges recently measured for the fp shell in the neutron deficient nuclei [42] was found to introduce staggering of the $B(E2)$ values in Ti isotopes which lowers the value for $N = 32$ almost to the experimental result [43]. The same experimental values of effective charges were used for the Cr isotopes when calculating $B(E2)$ values with KB3G. The result is shown in Fig. 3 as $\mathrm{KB3G_{mod}}$ curve. Although the staggering is observed as well, the general agreement between calculation and experiment did not improve. Nevertheless, this latest analysis proves that the indirect measurement of Cr or Ti isotopes does not give an unambiguous answer about a possible $N = 32, 34$ sub-shell closure and only studies of the respective Ca isotopes will address the problem directly.

6. Summary

The RISING project exploiting high-resolution γ-ray spectroscopy of nuclei far from stability proved to be very effective in providing new nuclear structure information in various campaigns. In particular the question of monopole driven shell structure at $N = 32, 34$ was addressed in the fast beam campaign. The final conclusion on the sub-shell closure in this region will be provided with a direct measurement of the transition probabilities in Ca isotopes. New results from Coulomb excitation were provided as well for ^{108}Sn [6] which shed light on the polarization of the ^{100}Sn core, and ^{134}Ce and ^{136}Nd [7]. The first results of the GDR measurement in ^{68}Ni are to be disclosed [28]. In the g-RISING and stopped beam campaign a wide range of nuclei was investigated yielding g-factors in neutron rich Sn isotopes [9] and newly identified isomeric states in ^{54}Ni [15], ^{82}Nb [12], ^{86}Tc [11], ^{130}Cd, ^{131}In [16], and ^{204}Pt [13]. The future campaign employing an active stopper foresees measurements of β-delayed γ rays.

This work is sponsored by the Polish Ministry of Science and Higher Education (grants 1-P03B-030-30 and 620/E-77/SPB/GSI/P-03/DWM105/ 2004–2007), the German Federal Ministry of Education and Research (grant 06KY205I) and by EURONS (European Commission contract No. 506065).

REFERENCES

[1] J. Eberth *et al., Nucl. Instrum. Methods* **A369**, 135 (1996).

[2] H. Geissel *et al., Nucl. Instrum. Methods* **B70**, 286 (1992).

[3] RISING Letter of Intent, `http://www-aix.gsi.de/~wolle/EB_at_GSI`.

[4] H.J. Wollersheim *et al., Nucl. Instrum. Methods* **A537**, 637 (2005).

[5] A. Bürger *et al., Phys. Lett.* **B622**, 29 (2005).

[6] A. Banu *et al., Phys. Rev.* **C73**, 061305(R) (2005).
[7] T. Saito *et al.*, submitted to *Phys. Rev.* **C**.
[8] P. Doornenbal *et al.*, submitted to *Phys. Lett.* **B**.
[9] G. Neyens *et al., Acta Phys. Pol. B* **38**, 1237 (2007) these proceedings.
[10] S. Pietri *et al., Acta Phys. Pol. B* **38**, 1255 (2007) these proceedings.
[11] A. Garnsworthy *et al., Acta Phys. Pol. B* **38**, 1256 (2007) these proceedings.
[12] L. Caceres *et al., Acta Phys. Pol. B* **38**, 1271 (2007) these proceedings.
[13] S. Steer *et al., Acta Phys. Pol. B* **38**, 1283 (2007) these proceedings.
[14] A. Myalski *et al., Acta Phys. Pol. B* **38**, 1277 (2007) these proceedings.
[15] D. Rudolph *et al.*, to be published.
[16] A. Jungclaus, M. Górska, M. Pfützner, *et al.*, to be published.
[17] E. Caurier *et al., Rev. Mod. Phys.* **77**, 427 (2005).
[18] J. Dobaczewski *et al., Phys. Rev. Lett.* **72**, 981 (1994).
[19] B. Pfeiffer *et al., Nucl. Phys.* **A693**, 282 (2001).
[20] T. Otsuka *et al., Phys. Rev. Lett.* **87**, 082502 (2001).
[21] H. Grawe, *Acta Phys. Pol. B* **34**, 2277 (2003).
[22] S. Lenzi *et al., Phys. Rev. Lett.* **87**, 122501 (2002).
[23] N. Pietralla *et al., Phys. Rev. Lett.* **83**, (1999) 1303.
[24] C. Fransen*et al., Phys. Lett.* **B508**, (2001) 219.
[25] A. Andreyev *et al., Nature* **405**, 430 (2000).
[26] D. Guillemaud-Mueller *et al., Nucl. Phys.* **A426**, 37 (1984).
[27] D. Cortina-Gil *et al., Phys. Rev. Lett.* **93**, 062501 (2004).
[28] A. Bracco, *Acta Phys. Pol. B* **38**, 1229 (2007) these proceedings.
[29] R. Lozeva *et al., Acta Phys. Pol. B* **36**, 1245 (2005).
[30] J. Ebert *et al., Prog. Part. Nucl. Phys.* **46**, 389 (2001)
[31] A. Maj *et al., Nucl. Phys.* **A571**, 185 (1994).
[32] J. Grębosz, *Comput. Phys. Commun.* (2006), in press.
[33] H. Grawe, *Springer Lect. Notes Phys.* **651**, 33 (2004).
[34] H. Grawe *et al., Eur. Phys. J.* **A25**, 357 (2005).
[35] H. Grawe *et al., Eur. Phys. J.* **A27**, 557 (2006).
[36] T. Otsuka *et al., Phys. Rev. Lett.* **95**, 232502 (2005).
[37] D.C. Dinca *et al., Phys. Rev.* **C71**, 041302 (2005).
[38] E. Caurier *et al., Eur. Phys. J.* **A15**, 145 (2002).
[39] M. Honma *et al., Phys. Rev.* **C69**, 034335 (2004).
[40] M. Honma *et al., Eur. Phys. J.* **A25**, 499 (2005).
[41] P. Reiter *et al.*, to be published.
[42] R. du Rietz *et al., Phys. Rev. Lett.* **93**, 222501 (2004).
[43] A. Poves *et al., Phys. Rev.* **C72**, 047302 (2005).